Dynamical System Theory of Flow Instability Using the Impulse and the Frequency Response Approaches

Tapan K. Sengupta , **Soumyo Sengupta** **and Prasannabalaji Sundaram**

Abstract We study the causal relation in a fluid dynamical system, for the impulse and frequency response approaches as instability theories and corresponding experiments. The zero-pressure-gradient (ZPG) boundary layer is analyzed to find complementary aspects of these approaches. The drawbacks of instability study are in formulating it as a homogeneous system. Another difficulty for the instability is in classifying it for either temporal or spatial growth. When viscous effects were included in the spatial theory, it predicted wave solution (known as Tollmien–Schlichting (TS) *waves*), which left many scientists unconvinced. Experimental verification remained difficult as instability does not require explicit excitation, and dependence on background noise makes experiment non-repeatable. The classic experiment of Schubauer and Skramstad for the boundary layer (J Aero Sci 14(2), 69–78, [24]) excited a monochromatic source inside to obtain spatially growing TS *waves*—considered as the frequency response of the boundary layer. In contrast, Gaster and Grant (Proc R Soc A 347(1649), 253–269, [13]) tried to create TS *waves* by a localized impulse excitation and ended up creating a wave-packet by the impulse response of the dynamical system. Here, we focus mainly on the impulse response of the ZPG boundary layer using Bromwich contour integral method (BCIM) developed by the authors for spatio-temporal growth of disturbance field in creating spatio-temporal wave-front (STWF). The main achievement of BCIM is in identifying the cause for the creation of STWF by both the approaches.

Keywords Impulse response · Frequency response · Bromwich contour integral method

T. K. Sengupta (✉) · P. Sundaram
High Performance Computing Laboratory, Department of Aerospace Engineering, Indian Institute of Technology Kanpur, Kanpur, Uttar Pradesh 208016, India
e-mail: tksen@iitk.ac.in

S. Sengupta
Graduate student, CERFACS, 31100 Toulouse, France

1 Introduction

One of the principal tenets in developing dynamical system theory is to study the relationship between cause and effects. This is true for a fluid dynamical system characterized by large degrees of freedom, as compared to other dynamical systems in many fields of physics. While experimental verification of any theory is imperative, however, this is a difficult task for theories of instabilities. This is because instability theories rely on the omnipresent imperceptible ambient disturbances to produce the response which is difficult to quantify. Mathematically, the instability problem is posed as the output of a system governed by a homogeneous differential equation, for homogeneous boundary and initial conditions. Implicit in this scenario is the requirement of an equilibrium state, in which the imperceptible omnipresent disturbance resides and draws energy for its growth. For example, flow past a circular cylinder displays unsteadiness above a critical Reynolds number (based on oncoming flow speed and diameter of the cylinder), even when one is considering uniform flow over a perfectly smooth cylinder. While this can be rationalized for experimental investigation, where the prevalence of background disturbances cannot be ruled out, the situation is far from straightforward for computational efforts. Roles of various numerical sources of error triggering instability for uniform flow past a smooth circular cylinder are complicated. This issue has been dealt in [31]. Inability to compute the equilibrium flow past a circular cylinder is due to the presence of adverse pressure gradient experienced by the flow on the lee side of the cylinder.

The situation is equally difficult for the ZPG flow over a flat plate. As the equilibrium flow is obtained with significant precision, it is possible to study the ZPG flow past a flat plate as a receptivity problem, as has been done experimentally to study the existence of TS *waves* by Schubauer and Skramstad [24], where the disturbances were effectively created by a vibrating ribbon inside the boundary layer. The computations have been done with varying degrees of success in [12, 3, 6, 7, 20, 29, 39] for 2D and 3D instability routes, with results improving with advent of better computers and numerical methods. Early results obtained in small computational domain managed to show TS wave-packets (and not waves), but starting with the theoretical finding of STWF due to a linear mechanism [32] along with TS wave-packet has completely changed our perception of the field, both in terms of theoretical and computational approaches.

While the experiment in [24] virtually rescued the theoretical instability studies, it is necessary to understand the motivation of that experiment. Concomitant with the developed spatial instability studies by solving Orr–Sommerfeld equation (OSE) (as given in [10, 27]), the boundary layer was excited by a monochromatic localized source, and hence, this can be termed as the frequency response of the boundary layer. In the experiment, the authors could not create TS *waves* by acoustic excitation, and this drew the attention on the subject of receptivity of equilibrium flows to different types of input to the system. As the existence of TS wave-packet cannot be demonstrated outside the strict confines of the laboratory, Gaster and Grant [13] studied the ZPG boundary layer excited by a localized impulse. Mathematically,

this is equivalent to using an input, which is a delta function in space and time, and the results provide the impulse response of the dynamical system. Interestingly, this experiment produced a wave-packet, which can be identified with the STWF found in [32]. It is noted that the search for STWF was sought in other branches of physics, with early efforts recounted in Brillouin [8] for electromagnetic wave propagation and by Bers [2] in plasma physics. Unfortunately, the authors in [13] thought that the impulse response was an ensemble of TS *waves*, which can be obtained by spatial instability theory for a parallel boundary layer, which was summed for the eigenfunctions with empirical weights. In a recent numerical study, Bhaumik and Sengupta [4] have shown the creation of the STWF by solving the complete Navier–Stokes equation (NSE) with an accurate numerical method. The authors identified the impulse response as the STWF, which is the building block that explains diverse physical and geophysical events, such as transition to turbulence, rogue waves and tsunamis. The role of STWF in creating transition to turbulence via frequency response route has been conclusively established in [3, 29, 30]. There are many efforts [19, 37] which have talked about transient growth, algebraic growth, as alternative routes of transition, without involving TS *waves*.

Thus, it is essential to bridge the theoretical gap between the impulse and the frequency response of a dynamical system, which are used in theoretical and experimental studies. Here, the results for ZPG boundary layer are used to theoretically explain the common elements of the impulse and frequency responses. In the context of flow instability, the difference between the two responses continues to baffle the research community. The primary goal of the present research is to theoretically explain from the solution of OSE, the existence of STWF and its ubiquitous role in manifesting unsteady effects, even when the excitation is imposed impulsively once, which continues to grow indefinitely. Such an exercise can show the presence of STWF even when the amplitude of the STWF is small at the onset. We note that the STWF was found due to a change of point of view when flow instability was solved for generic spatio-temporal growth.

In the beginning, Orr and Sommerfeld [21, 34] proposed OSE without any qualifier on the disturbance growth, whether it is in space or in time. When Rayleigh's theorem for temporal growth failed to explain the instability of ZPG boundary layer [10], it was assumed that the growth must be in space. Although Heisenberg, Tollmien and Schlichting [10, 17, 23, 27, 36] solved the temporal instability for OSE, the results were interpreted as growth in space, using the growth in time to growth in space, using the group velocity [8, 27]. With the advent of computers, OSE has been solved by few methods for stiff differential equations. Of all the methods, the most reliable one appears to be the compound matrix method (CMM) described in [10, 26, 27]. In Sengupta [25], CMM was used along with discrete fast Fourier transform (DFFT) to solve the problem corresponding to the experiment of [24] using the signal-problem assumption. This is the first numerical solution, while theoretical conjectures exist in [1, 14, 15].

Here, we explain how the STWF is created for different start-up conditions by BCIM in solving OSE for a 2D response field. The corresponding solution of NSE has been shown for impulsive and non-impulsive start-ups in [5]. The formulation

of the problem is shown in Sect. 2. This is followed by a description of the utility
of the signal problem in Sect. 3. Next, the impulse response for the ZPG boundary
layer is shown in Sect. 4, for three different Reynolds numbers, based on displace-
ment thickness. The frequency response cases are shown next in Sect. 5, for three
streamwise exciter locations, with identical physical frequency of excitation, to con-
firm with the parallel flow approximation in solving OSE. In the following Sect. 6,
we describe the receptivity of ZPG boundary layer, when the input has no specific
time scale imposed, while the time variation of input corresponds to a Heaviside
function, a ramp and a rapidly varying function, but with smooth variation at the
onset and the final state. To emphasize the importance of boundary layer growth and
the corresponding shortcoming of parallel flow approximation, the case of frequency
response described in Sect. 5 by solving OSE is computed again by solving NSE in
Sect. 7. The paper closes with a summary and conclusion.

2 Formulation of the Impulse and the Frequency Response

The schematic of the problem is shown in Fig. 1a in the physical plane, while it
is solved in the spectral plane, involving streamwise wavenumber (α) and circular
frequency (ω_0). For the 2D problem, the response is calculated for the linearized field
following the governing OSE given by

$$D^4\phi = i\tilde{R}e\big[(\alpha U(\tilde{y}) - \omega_0)D^2\phi - \alpha U''(\tilde{y})\phi\big] \tag{1}$$

where $D^2 = \frac{d^2}{d\tilde{y}^2} - \alpha^2$, $\tilde{R}e = \frac{U_e\delta^*}{\nu}$. Here, the displacement thickness at the exciter
location has been used as the length scale, while the free stream speed is used as
the velocity scale. The time scale is derived with the help of these two scales. The
disturbance stream function is given by its spectral transform as

$$\bar{\psi} = \underset{\alpha_{Br}}{\int} \underset{\omega_{Br}}{\int} \phi(\alpha, \tilde{y}, \omega_0)e^{i(\alpha\tilde{x} - \omega_0 t)}d\alpha d\omega_0 \tag{2}$$

which is solved for both the signal and spatio-temporal problems using BCIM. The
difference between these two lies in choosing integration contours in the spectral
plane, in the respective strip of convergence—known as the Bromwich contour [22,
27, 38]. Here, the response to wall excitation is studied for three types of excitation
fields: (i) Case-I—where the input is simply a product of delta functions in space
and time that represents the pure impulse response. The other cases are shown in
Fig. 1b, with the impulsive start represented by the Heaviside function (Case-II) and
the other represents a non-impulsive start (Case-III) given by

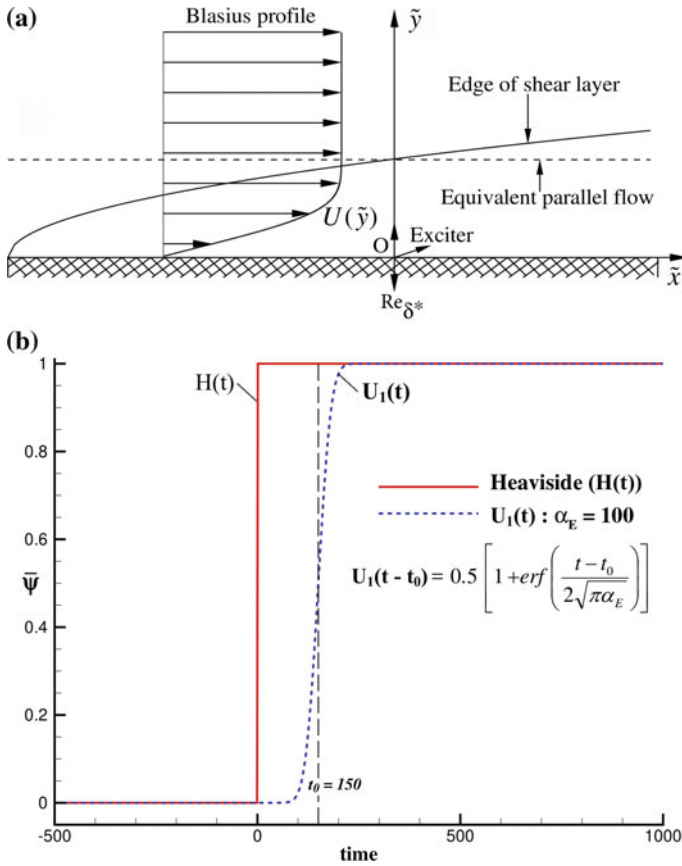$$U_1(t - t_0) = 0.5\left[1 + \text{erf}\left(\frac{t - t_0}{2\sqrt{\pi}\alpha_E}\right)\right] \tag{3}$$

Fig. 1 a Schematic of the computation domains for the wall excitation of an equivalent parallel flow given by Blasius profile at a location indicated by the dashed line and **b** the envelope of the time-dependent excitations given by the Heaviside function ($H(t)$) and an error function ($U_1(t)$), triggered at the indicated times; $t = 0$ for $H(t)$ and $t = t_0$ for $U_1(t - t_0)$

which is related to the error function. One can study the impulse and frequency response cases, where $H(t)$ and $U_1(t)$ represent the envelope for the amplitude of input disturbance stream function, $\bar{\psi}$. If the excitation frequency is $\bar{\omega}_0$, then the excitation for the frequency response case is given by $\bar{\psi} e^{-i\bar{\omega}_0 t}$. Here, we have reported only one frequency response case, which is started impulsively using $H(t)$. We have also studied cases, where the dynamical system is excited by inputs, as shown in Fig. 1b without any imposed time scale, which will be termed as non-oscillatory transient cases. Additionally, a case of ramp start (Case-IV) is also studied which is non-oscillatory. Note that when α_E approaches zero in Eq. (3), one recovers the Heaviside function, $H(t)$. Also in Fig. 1b, the non-impulsive case $U_1(t - t_0)$ becomes nonzero from $t = 0$ onwards, while it is centered around t_0. For this reason, the

Fourier transform has been calculated, using time-scaling, frequency and time-shift theorems of Fourier transform [27].

We want to highlight the fact that for the frequency response case, the finite start-up with Heaviside function introduces all possible circular frequencies. Even in the case where $U_1(t)$ is characterized by α_E, with a small value, one excites a wide range of frequencies, apart from $\bar{\omega}_0$, for the frequency response case. For an unstable system, it is not necessarily guaranteed that the response will be dictated by $\bar{\omega}_0$ only. Thus, for the study of instability, there are hardly any differences between impulse and frequency responses, as both the cases are excited by wide-band input by finite start-up.

In the signal problem, it is assumed that the response is at the frequency of excitation, $\bar{\omega}_0$, and as a consequence, the frequency is fixed, i.e., $\omega_0 = \bar{\omega}_0$, and one solves Eq. (1) along the Bromwich contour in $\alpha (= \alpha_r + i\bar{\alpha}_i)$-plane only. Choice of constant $\bar{\alpha}_i$ facilitates use of DFFT for the inverse transform. The Bromwich contours used in BCIM are shown in Fig. 2, with the choice of contour dictated by the position of various eigenvalues in complex α and ω_0 planes, with details explained in [16, 27, 28].

As noted for unstable systems, the signal-problem assumption is incorrect. To solve the problems correctly, the BCIM was proposed [27, 28], where the dynamical system picks up the correct space-time scales for the fixed $\tilde{Re}$, consistent with the physical dispersion relation. After solving Eq. (1) along the Bromwich contours in the complex α- and ω_0-planes, as shown in Fig. 2, one performs double inverse transforms to recover the response field in the physical plane. Using BCIM, the STWF was noted first in [32], which was shown to cause 2D turbulence in [29, 30] and 3D turbulence in [3], in the framework of experiments performed using the frequency response approach. The existence of STWF by the impulse response has also been shown by solving 3D NSE for 3D routes of transition in [4, 35].

In the present work, the linearized problem is solved theoretically and computationally by considering different impulse and frequency response approaches. Only
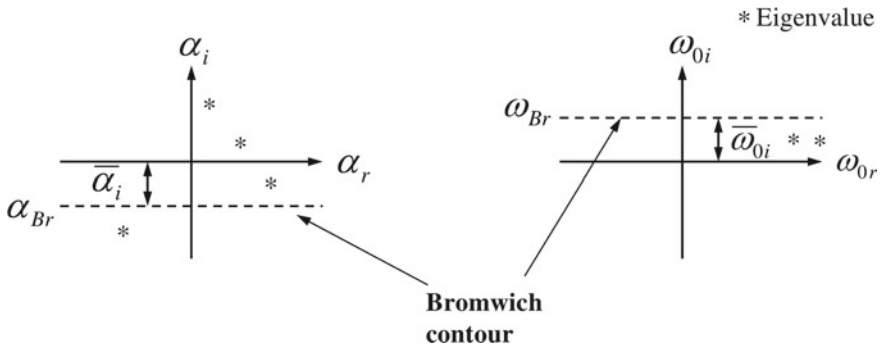

Fig. 2 Bromwich contours used here have been shown in complex α and ω_0-planes for the BCIM approach. For signal problems, only the contour in α-plane is used

one frequency response case is included here to demonstrate the difference between solution of OSE by BCIM and by direct simulation of NSE.

3 The Utility of the Signal Problem

Results of Eq. (1) have been obtained with the signal-problem assumption for the first time in [25] using CMM [27]. The same method has been used here, by considering the height of the domain in the wall-normal direction given by the similarity variable used in Blasius solution as $\eta_{\max} = 12$ with 3000 points. Along the Bromwich contour (α_{Br}), 8192 points are taken, for which Eq. (1) is solved, along with $\bar{\alpha}_i = -0.008$. While it has been reasoned above that the signal problem is inconsistent for instability studies, and instead, one should treat these as spatio-temporal growth problem, as in [27, 28, 32] to study frequency response cases. Thus, one should solve Eq. (1) for any type of excitation implied in Eq. (3), along the Bromwich contours shown in Fig. 2. Finally, double inverse Fourier transform is performed to obtain $\bar{\psi}$, as given in Eq. (2). This is the BCIM technique followed in [27, 28, 32], which led to the finding of the STWF. It is readily noted in BCIM that one needs to solve the signal problem, for every point along the Bromwich contour, ω_{Br} in the ω_0-plane.

In Fig. 3, $\bar{\psi}$ is plotted for three different cases with $\tilde{Re}$ and $\bar{\omega}_0$ combinations given by (1000, 0.1), (1500, 0.15) and (2000, 0.20), such that the physical frequency $F = \frac{\bar{\omega}_0}{\tilde{Re}}$ remains the same. The results are shown at a height which is close to the inner maximum of the disturbance field. The solution is determined by the instability
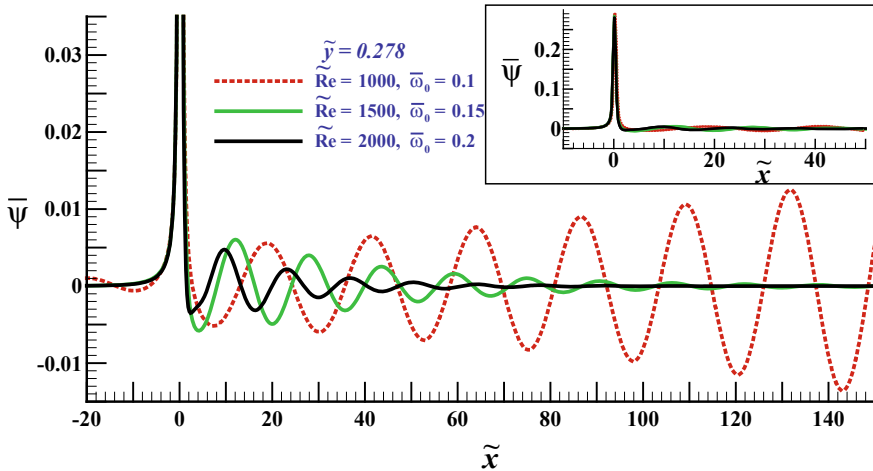

Fig. 3 Signal-problem solution for three representative $\tilde{Re}$ values, with results shown at the indicated height, $\tilde{y} = 0.278$. The non-dimensional frequencies are so chosen that one is tracking the same physical frequency. The Bromwich contour in α-plane is at $\bar{\alpha}_i = -0.008$, and α_r ranges from -4π to $+4\pi$, with 8192 points

property of the Blasius boundary layer, as given by the spatial analysis. Thus, the first combination shows growing TS wave. These results show the unique feature of receptivity analysis, in the form of a local solution in the vicinity of the exciter at $\tilde{x} = 0$, whose full view is shown in the inset, on the top right. These features of solution for the signal problem is noted in the solution using BCIM, except that the STWF is not seen, as one noted the STWF from the spatio-temporal solution of OSE and NSE in [28, 29, 32].

4 The Impulse Response of the Blasius Boundary Layer

In studying the spatio-temporal dynamics for the Blasius boundary layer, we first consider the case of pure impulse, with the wall excitation given by

$$\bar{\psi}(\tilde{x}, 0, t) = \delta(\tilde{x})\delta(t) \tag{4}$$

This is the type of wall excitation investigated in [13]. The results are obtained here by solving Eq. (1), for the input given by Eq. (4), using BCIM along the Bromwich contours, α_{Br} and ω_{Br}, using 8192 and 2048 points, respectively. The Bromwich contours are parallel to the real axis, located below at $\bar{\alpha}_i = -0.008$ in α-plane and above at $\bar{\omega}_{0i} = 0.01$ in the ω_0-plane. The height of the domain in the wall-normal direction is same, as that has been used in the signal problem. For each ω_0, one solves an equivalent signal problem, as described in the previous section. The results shown in Fig. 4 are for three $\tilde{R}e$ indicated in the frame. At the location of the exciter ($\tilde{x} = 0$), one notices the local solution which rapidly decays with time. However, in this case, one does not also see the TS wave, and instead the STWF is noted, that convects in the downstream direction, at nearly the same speed. For $\tilde{R}e = 1000$, the STWF appears at a downstream location, despite the fact that the excitation for this case is applied at the most upstream station. These results here are shown from the solution of OSE, which requires the parallel flow approximation, while the solution of 3D NSE has been shown in [4, 35]. In [13], it was assumed that the STWF is a weighted sum of TS *waves* created by the corresponding signal problem. The present solution not only shows the superiority of BCIM but also establishes the correct interpretation of STWF as the basic unit process of disturbance growth for the equilibrium flow arising as the impulse response.

5 The Frequency Response of the Blasius Boundary Layer

It has been noted already that the frequency response of a dynamical system is a misnomer for a physically unstable system, as the unstable modes are going to be
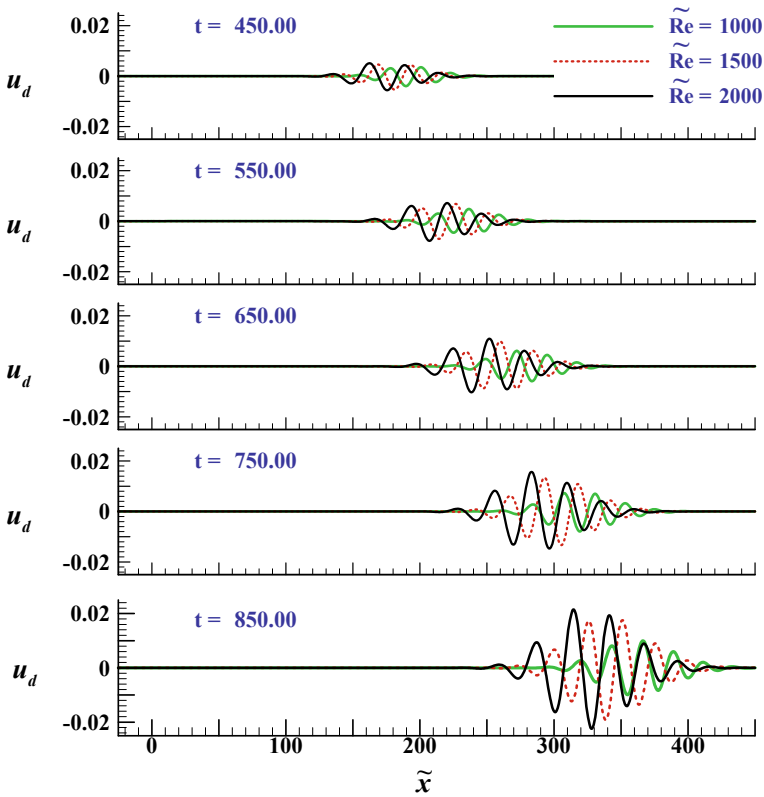
Fig. 4 Impulse response of the Blasius boundary layer to excitation as given by Eq. (4) for three representative $\tilde{R}e$ values, with results shown at the indicated height, $\tilde{y} = 0.278$. The Bromwich contour in α-plane is at $\bar{\alpha}_i = -0.008$, and α_r ranges from -4π to $+4\pi$ with 8192 points, and in the ω_0-plane the Bromwich contour is placed at $\bar{\omega}_i = 0.01$, and ω_{0r} varying from $-\pi/2$ to $+\pi/2$ with 2048 points

dominant, as compared to the forced response at the excitation frequency. Historically, this wrong perception arose due to adoption of spatial instability theory for fluid flow, in which one looks for spatial growth at the imposed frequency, associated with the signal-problem assumption. We have already noted in describing the various wall excitation cases that the finite-time start-up excites all possible circular frequencies, and the roles of various modes of transient variation have been noted in the previous section on impulse response. In this case the wall excitation is given by

$$\bar{\psi}(\tilde{x}, 0, t) = \delta(\tilde{x})\bar{\psi}_0 e^{-i\bar{\omega}_0 t} \tag{5}$$

where $\bar{\psi}_0 = H(t)$ or $U_1(t)$ with a chosen value of α_E, depending on whether the start-up is impulsive (as given by Heaviside function) or non-impulsive (as given by

error function-type variation, with $U_1(t)$). The frequency response with impulsive start given by Heaviside function has been solved originally in [28] for a case with $\tilde{Re} = 1000$ and $\bar{\omega}_0 = 0.1$, which has been pronounced as spatially unstable. Here, we have solved the same problem, with significantly higher number of points in $\tilde{x}$- and $\tilde{y}$-directions.

The results shown in Fig. 5 are for the spatially unstable case ($\tilde{Re} = 1000$ and $\bar{\omega}_0 = 0.10$) solved by BCIM. In the depicted solution, apart from the local solution, the TS wave-packet and the STWF are also present. It is not readily apparent that there exists the STWF, as it was also not identified in [28], where this set of results were presented for the first time. For this spatially unstable case, the TS wave-packet and the STWF are fused together in the displayed solution of OSE, shown for the indicated times. We would like to emphasize that this typical structure of blended TS wave-packet and STWF is a consequence of the parallel flow assumption used to formulate and solve OSE. Otherwise, the solutions of OSE for other stable cases, as
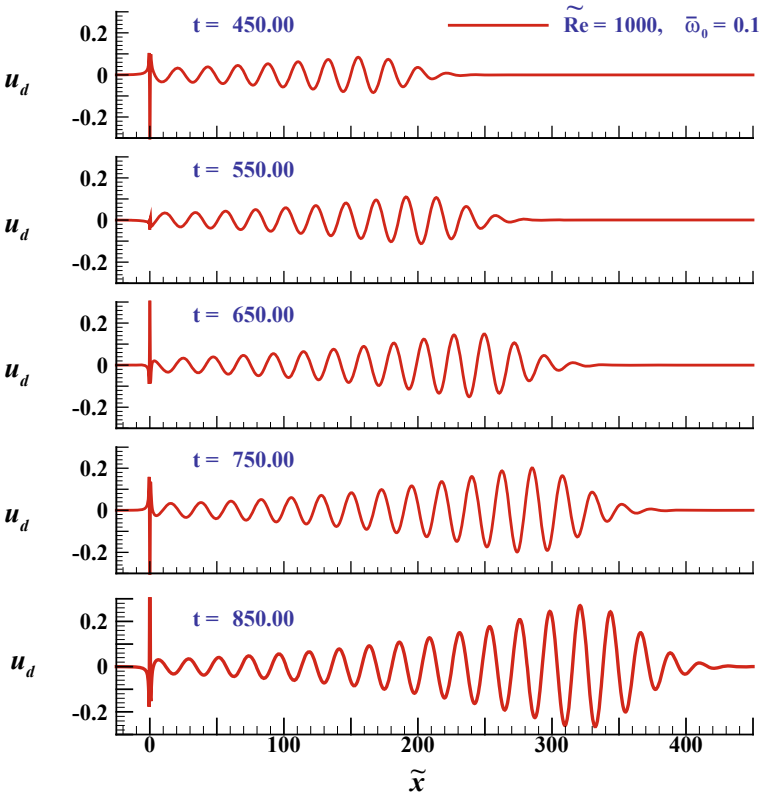

Fig. 5 Frequency response of the Blasius boundary layer to excitation as given by Eq. (5) for $\tilde{Re} = 1000$ and $\bar{\omega}_0 = 0.1$, with results shown at $\tilde{y} = 0.278$. The Bromwich contours are the same used in Fig. 4

will be shown later, display the separation of TS wave-packet and the STWF. Later, when BCIM was used to investigate spatially stable cases in [32, 33], the presence of STWF was easily discerned, with the TS wave-packet is seen to decay with space, while STWF grows and convects downstream. Two such stable cases are shown here in Fig. 6 for the indicated parameters.

The emergence of TS wave-packet is clearly visible from the local solution in all the frames. The property of the TS wave-packet is dictated primarily by the spatial stability property of the OSE at the location of the exciter, and it is easy to rationalize the decay of the TS wave-packet. However, the STWF has the property of growth in space and time and has little to do with spatial theory properties. The propagation properties are the same, as seen in Fig. 4. Consistent with the parallel flow assumption, the solutions shown in Figs. 5 and 6 are for the same constant physical frequency (f), for which $\frac{\tilde{\omega}_0}{\tilde{Re}}$ remains constant, which in this case provides the non-dimensional physical frequency as $F = 2\pi f \nu / U_\infty^2$.
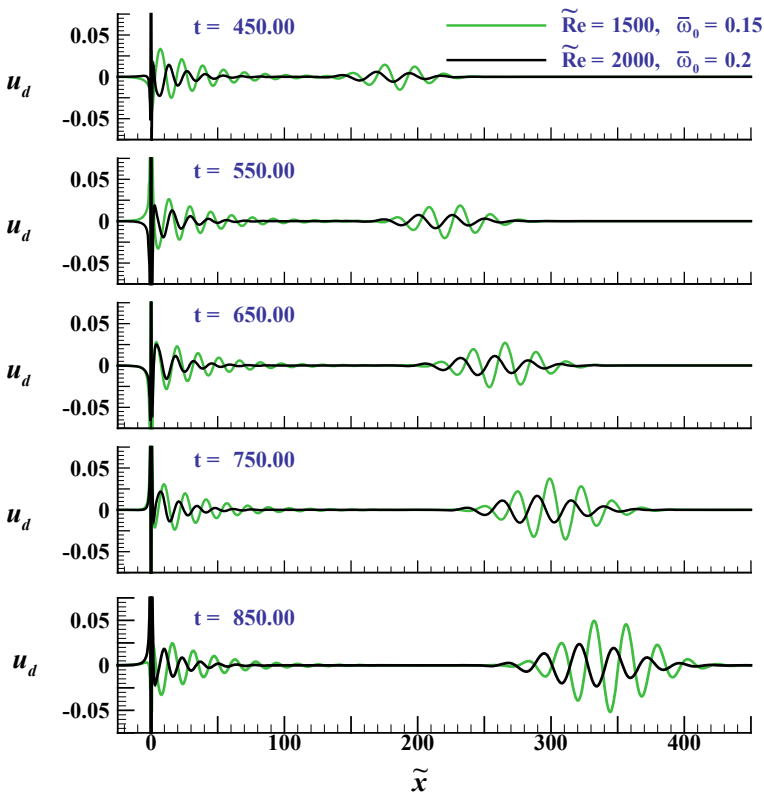

Fig. 6 Frequency response of the Blasius boundary layer to excitation as given by Eq. (5) for $\tilde{Re} = 1500$ and 2000, for $\bar{\omega}_0 = 0.15$ and 0.20, respectively. The results are shown at $\tilde{y} = 0.278$. The Bromwich contours are described in Fig. 4

6 Non-oscillatory Start-up Cases Solved by BCIM

Having noted the distinction between the impulse and the frequency response in the previous two sections, we note the absence of TS wave-packet for the former. At the same time, both cases have a local solution and STWF. However, the local solution for the impulse response is significantly smaller, and which furthermore rapidly decays with time. Thus, after some time, only the STWF will be the common link between the solutions of the impulse and the frequency response cases. It has been shown that the STWF is the precursor of transition to turbulence for 2D in [29] and 3D transition in [3, 4, 35]. It has also been shown that it is not necessary that STWF is created due to impulsive start for frequency response cases in [5]. The ever-growing STWF for both the impulse and frequency response cases shows that it is not necessary to impose any specific time scale to cause transition. However, imposition of time scale helps in creating TS wave-packets, which helps in transition for the frequencies which are closer to Branch-I of the neutral curve, where STWF is constantly fed by TS wave-packet and which does not remain stationary. These cases have been termed as interacting or I-type transition cases in [5]. Keeping this in view, next, we report response of Blasius boundary layer to wall excitations which are associated with a sudden jump used as the input, without any oscillation frequency associated with the input.

6.1 Impulsive Excitation at the Wall by a Heaviside Function

In this case, the exciter is placed at a location, where $\tilde{Re} = 1000$, and the input excitation is given by the Heaviside function. Given that the present investigation is for a linearized system, the amplitude of excitation is in non-dimensional form of unity value. Thus, the discussion here pertains to unit amplitude of excitation applied on the disturbance stream function, which can be scaled to the actual value of wall perturbation.

In Fig. 7, the streamwise component of disturbance velocity is shown as a function of streamwise distance at a height of $\tilde{y} = 0.278$, for the indicated time instants. In this case also, one can clearly observe the evolution of the STWF with space and time. The fact that the STWF is created by a delta and Heaviside function clearly establishes that transition to turbulence can be caused by such an impulsive excitation, as shown in Figs. 4 and 7. This clearly underlines the fact that for ZPG boundary layer, the transition to turbulence can be caused by the STWF without the presence of TS *waves* or wave-packets.
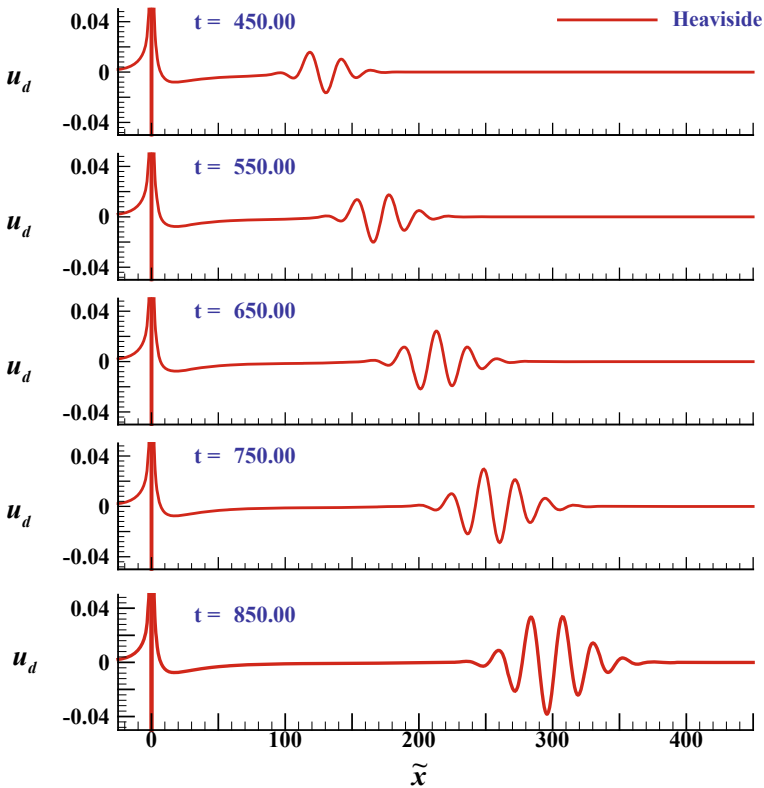
Fig. 7 Response of the Blasius boundary layer to excitation given by the Heaviside function for $\tilde{Re} = 1000$. Results are shown for $\tilde{y} = 0.278$. The Bromwich contours are as in Figs. 4, 5 and 6. The input is given in the form of unit disturbance stream function at the exciter location

6.2 Non-impulsive Excitation at the Wall Given by Ramp and Error Function

In these cases, we have used input disturbance stream function from Eq. (3) for the error function with $\alpha_E = 100$ and $t_0 = 150$, and the ramp function increases linearly from zero at $t = 0$ to unit value at $t = 300$. To solve OSE, the boundary conditions are obtained using DFFT of the time signal at the exciter. The results are obtained by solving OSE using BCIM, and Bromwich contours are chosen as before for the impulse and frequency response cases.

In Fig. 8, the streamwise component of disturbance velocity is shown as a function of streamwise distance for the two cases at the indicated times. We observe that these cases produce response fields which are one order of magnitude lower, as compared to the case shown in Fig. 7. Due to the faster growth rate of the error function excitation case, as compared to the ramp function case, the response field amplitude is higher
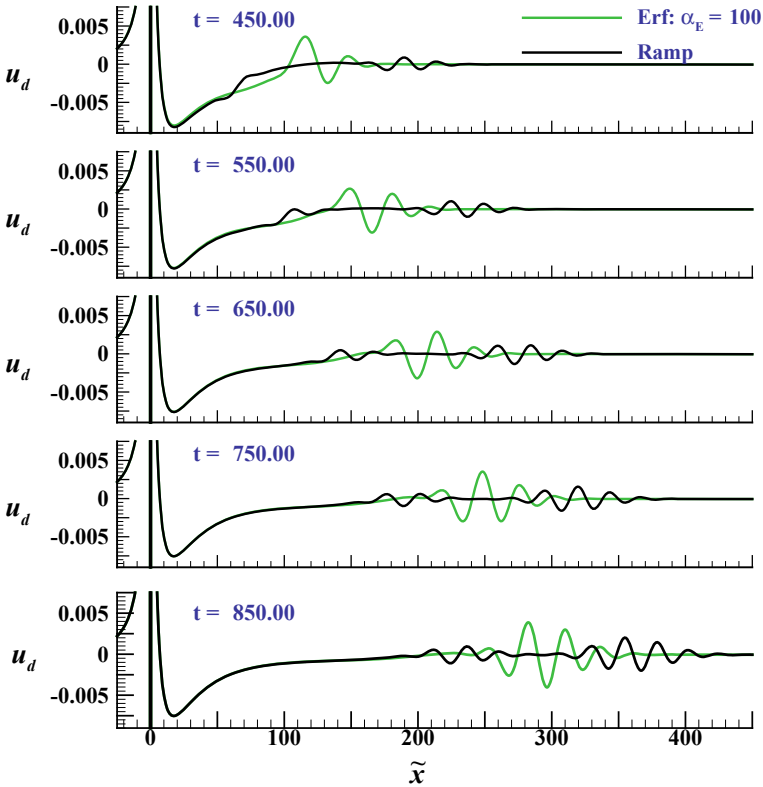
Fig. 8 Response of the Blasius boundary layer to excitation given by error function and ramp function for $\tilde{R}e = 1000$ during the time interval of $0 \leq t \leq 300$, with results shown for $\tilde{y} = 0.278$. The Bromwich contours are as in Figs. 4, 5 and 6. The input is given in the form of constant disturbance stream function at the exciter location

for the former. However, small is the approach of the input disturbance field to the same final value, one expects creation of the STWF, implying the ubiquitous nature of the STWF. Due to slope discontinuity during onset and terminal stage of the ramp start-up, one can see two distinct STWFs in the disturbance field as shown in Fig. 8. Given sufficient length and presence of wall shear, the STWF will grow eventually to cause transition to turbulence.

Although the response for the case of non-oscillatory Heaviside function is one order of magnitude higher than the other two cases, the spectrum of the response fields as shown in Fig. 9 indicates that the scales of the STWF for all the three cases are similar. One also notices that the STWF occurs not at a particular length scale but is a wide-band phenomenon centered around $\alpha_r \approx 0.3$ for the displayed time, $t = 450$. Subsequently, all the three cases amplify which is the universal feature of the STWF.
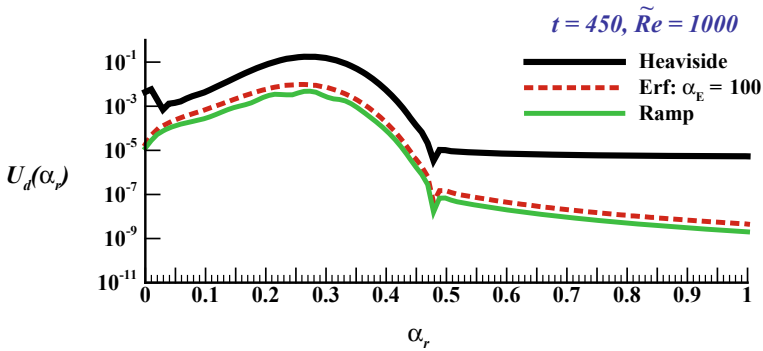
Fig. 9 Fourier transform of u_d for the three non-oscillatory input cases, whose responses are shown in Figs. 7 and 8 at the indicated time, $t = 450$

7 The Frequency Response Obtained from the Solution of the Navier–Stokes Equation

We have noted in Fig. 5 that the TS wave-packet and the STWF are together at all times. This led to confusion in [28], whereby the STWF was not recognized. Subsequently, when the spatial stable cases were solved by BCIM in [32, 33], one could distinguish between the TS wave-packet and the STWF, as also seen in Fig. 6. This particular feature for the spatially unstable cases is due to the parallel flow approximation, as was noted from the solution of NSE in [29].

The case considered in [29] was with a simultaneous blowing-suction strip extending from $\tilde{Re} = 656$–676, and such an excitation led to fully developed turbulence studied for different amplitude of excitation, displaying k^{-3} spectrum for u_d. For the case considered here in Fig. 5, we report the corresponding solution by solving NSE in Fig. 10.

We would like to point out that the scales used in representing the NSE are based on convection scales, while those used for OSE are viscous scales. For example, the viscous time scale is given by $T_{sc} = \frac{\delta^*}{U_\infty}$, whereas in solving the NSE, we have used a length scale (L), such that the corresponding Reynolds number is given by $Re_L = 10^5$ and the corresponding time scale is $T_c = \frac{L}{U_\infty}$. As a consequence, the ratio of the two time scales is given by $\frac{T_c}{T_{sc}} = \frac{Re_L}{\tilde{Re}}$. For the solution of NSE, the non-dimensional coordinates are given by x and y. From the top frame at $t_c = 25$, one can clearly observe that the STWF is distinctly different from the TS wave-packet. The solutions of OSE shown have extraordinarily high resolution as compared to the solution obtained by the NSE, because of the different time resolution of NSE and OSE. Thus, it is not possible to show solution of OSE corresponding to the top frame of Fig. 10 with the number of points taken in ω_0-plane. In Fig. 10, one notices continual growth and downstream propagation of the STWF, while the TS wave-packet appears to remain stationary, although this is a progressive wave, whose
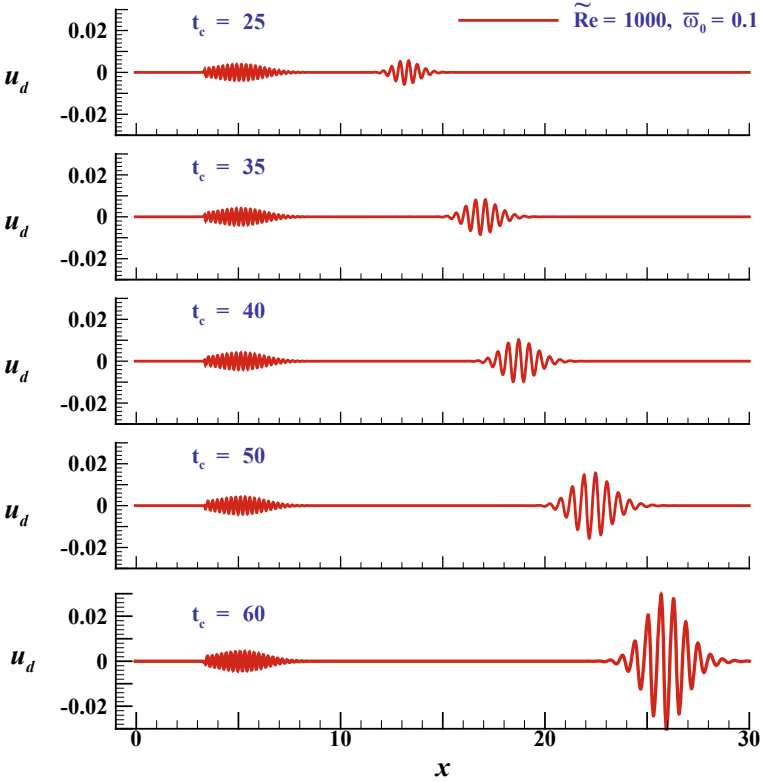
Fig. 10 Frequency response of the Blasius boundary layer to excitation as given by Eq. (5) with the exciter located where $\tilde{Re} = 1000$ for $\bar{\omega}_0 = 0.1$, and the results for u_d are shown at $y = 0.278$ for the indicated times

amplitude decays with downstream co-ordinate x. The observed stationary nature of the TS wave-packet is determined by the wave properties of the packet as determined by its growth and decay for the constant frequency wall excitation. The solution displayed in Fig. 10 is all during the linear growth stage of the STWF. The detailed 2D solution of similar cases has been reported in [29, 30].

8   Summary and Conclusion

Here, we have studied the impulse and frequency response cases to reconcile between the experiments reported in [24] (which has been termed as frequency response, as the input is provided at a fixed frequency consistent with the practice in spatial stability theory) and those in [13], where a wave-packet is created by a localized delta function excitation in space and time, as given in Eq. (4). The output of such an excitation can

be termed indeed as the impulse response. Such an experimental approach is used in [13] to provide help with understanding natural transition. In contrast, the theoretical TS *waves* have been created only in a strict laboratory setting with a monochromatic excitation at a fixed frequency. In real flows, transition to turbulence is often noted as a turbulent spot or puff [11, 18]. We have reasoned that even the so-called frequency response starts at a finite time, and therefore, such an excitation is also similar to impulse excitation, and we have investigated three different start-ups: Impulsive (as given by Heaviside function), non-impulsive with varying acceleration [as given by Eq. (3)] and a linear ramp function. Only in the frequency response case, the input [as given by Eq. (5)] produces TS wave-packet as obtained from the solution of Navier–Stokes equation in Fig. 10, which have also been reported in [29, 30].

For both the cases of the impulse and frequency responses, one notices the common elements of the local solution and the spatio-temporal wave-front (STWF) here from the solution of linearized analysis of Orr–Sommerfeld equation (OSE). However, for impulse response, the local solution is insignificantly smaller for the impulse response, and furthermore, the amplitude of which decays with time. The presented results are from the solution of governing Navier–Stokes equation (NSE) in its full form or in its linearized version of OSE. This is distinctly different from various other approaches reported in the literature [9, 19]. It has been shown in [3, 29, 32] that frequency response cases create STWF, which is the precursor of transition to turbulence obtained from the solution of OSE and NSE. For the impulse response case, the existence of STWF has been shown from the solution of NSE in [4, 35]. It is shown here from the solution of OSE for the input excitation given by strictly delta function in space and time. Apart from this, existence of STWF is also shown, when the input is given by a Heaviside function, linearly varying ramp function and an error function. All of these excitations have varying degree of time variation of the input excitation for impulsive and non-impulsive start-ups. While all of these demonstrate the creation of STWF, none of these show TS wave-packets. The spectra of the various STWFs shown in Fig. 9 show the universality of the STWF. It is also explained that for the spatially unstable case shown in Fig. 5, one does not see the distinct STWF due to parallel flow assumption, as the same case solved using NSE in Fig. 10 display the STWF and the TS wave-packet. However, in Fig. 6, one can clearly see the demarcated STWF from the decaying TS wave-packet. All of these observations lead us to conclude that the STWF is the precursor of transition for both the impulse and frequency responses for the boundary layer and is created by the linear mechanism, governed by OSE. This point of view perfectly blends with experimentally observed transition to turbulence for not only wall-bounded flows but also for internal flows and free shear layers.

References

1. Ashpis, D.E., Reshotko, E.: The vibrating ribbon problem revisited. J. Fluid Mech. **213**, 531 (1990)

2. Bers, A.: Physique des Plasmas. Gordon and Breach, New York, USA (1975)
3. Bhaumik, S., Sengupta, T.K.: Precursor of transition to turbulence: Spatiotemporal wave front. Phys. Rev. E **89**(4), 043018 (2014)
4. Bhaumik, S., Sengupta, T.K.: Impulse response and spatio-temporal wave-packets: the common feature of rogue waves, tsunami and transition to turbulence. Phys. Fluids **29**, 124103 (2017)
5. Bhaumik, S., Sengupta, T.K., Shabab, Z.A.: Receptivity to harmonic excitation following non-impulsive start for boundary layer flows. AIAA J. **55**(10), 3233–3238 (2017)
6. Borrell, G., Sillero, J.A., Jiménez, J.: A code for direct numerical simulation of turbulent boundary layers at high Reynolds numbers in BG/P supercomputers. Comput. Fluids **80**, 37–43 (2013)
7. Breuer, K.S., Cohen, J., Haritonidis, J.H.: The late stages of transition induced by a low-amplitude wavepacket in a laminar boundary layer. J. Fluid Mech. **340**, 395–411 (1997)
8. Brillouin, L.: Wave Propagation and Group Velocity. Academic press, New York, USA (1960)
9. Chomaz, J.-M.: Global instabilities in spatially developing flows: non-normality and nonlinearity. Annu. Rev. Fluid Mech. **37**, 357–392 (2005)
10. Drazin, P.G., Reid, W.H.: Hydrodynamic Stability. Cambridge University Press, UK (1981)
11. Emmons, H.W.: The laminar-turbulent transition in a boundary layer-Part I. J. Aeronaut. Sci. **18**(7), 490–498 (1951)
12. Fasel, H., Konzelmann, U.: Non-parallel stability of a flat plate boundary layer using the complete Navier-Stokes equation. J. Fluid Mech. **221**, 331–347 (1990)
13. Gaster, M., Grant, I.: An experimental investigation of the formation and development of a wave packet in a laminar boundary layer. Proc. Royal Soc. A **347**(1649), 253–269 (1975)
14. Gaster, M.: On the generation of spatially growing waves in a boundary layer. J. Fluid Mech. **22**, 433 (1965)
15. Gaster, M.: Growth of disturbances in both space and time. Phys. Fluids **11**, 723–727 (1968)
16. Gaster, M., Sengupta, T.K.: The generation of disturbances in a boundary layer by wall perturbations: the vibrating ribbon revisited once more. In: Instabilities and Turbulence in Engineering Flows, Kluwer Academic Publisher, Dordrecht, The Netherlands (1993)
17. Heisenberg, W.: Über stabilität und turbulenz von flüssigkeitsströmen. Ann. Phys. Lpz. **379**, 577–627 (1924). (Translated as On stability and turbulence of fluid flows. NACA Tech. Memo. Wash. No 1291, 1951)
18. Hof, B., Doorne, C.W.H.V., Westerweel, J., Nieuwstadt, F.T.M., Faisst, H., Eckhardt, B., Wedin, H., Kerswell, R.R., Waleffe, F.: Experimental observation of nonlinear traveling waves in turbulent pipe flow. Science **305**(5690), 1594–1598 (2004)
19. Huerre, P., Monkewitz, P.A.: Absolute and convective instabilities in free shear layers. J. Fluid Mech. **159**, 151–168 (1985)
20. Kloker, M.J.: A robust high-resolution split-type compact FD scheme for spatial direct numerical simulation of boundary-layer transition. Appl. Sci. Res. **59**(4), 353–377 (1997)
21. Orr, McF.W.: The stability or instability of the steady motions of a perfect liquid and of a viscous liquid, Part I: A perfect liquid. Part II: A viscous liquid. Proc. Roy. Irish Acad., *A27*, 9–138 (1907)
22. Papoulis, A.: Fourier Integral and Its Applications. McGraw Hill, New York, USA (1962)
23. Schlichting, H.: Zur entstehung der turbulenz bei der plattenströmung. Nachr. Ges. Wiss. Goettingen, Math.-Phys. Kl., **42**, 181–208 (1933)
24. Schubauer, G.B., Skramstad, H.K.: Laminar boundary layer oscillations and the stability of laminar flow. J. Aero. Sci. **14**(2), 69–78 (1947)
25. Sengupta, T. K.: Impulse response of laminar boundary layer and receptivity. In: 7th International Conference on Numerical Methods In Laminar and Turbulent Flows. Pineridge Press (1991)
26. Sengupta, T.K.: Solution of the Orr-Sommerfeld equation for high wave numbers. Comput. Fluids **21**(2), 301–303 (1992)
27. Sengupta, T.K.: Instabilities of Flows and Transition to Turbulence. CRC Press, Taylor & Francis Group, Florida, USA (2012)

28. Sengupta, T.K., Ballav, M., Nijhawan, S.: Generation of Tollmien—Schlichting waves by harmonic excitation. Phys. Fluids **6**(3), 1213–1222 (1994)
29. Sengupta, T.K., Bhaumik, S.: Onset of turbulence from the receptivity stage of fluid flows. Phys. Rev. Lett. **154501**, 1–5 (2011)
30. Sengupta, T.K., Bhaumik, S., Bhumkar, Y.: Direct numerical simulation of two-dimensional wall-bounded turbulent flows from receptivity stage. Phys. Rev. E **85**(2), 026308 (2012)
31. Sengupta, T.K., Singh, N., Suman, V.K.: Dynamical system approach to instability of flow past a circular cylinder. J. Fluid Mech. **658**, 82–115 (2010)
32. Sengupta, T.K., Rao, A.K., Venkatasubbaiah, K.: Spatio-temporal growing wave fronts in spatially stable boundary layers. Phys. Rev. Lett. **96**(22), 224504–1–4
33. Sengupta, T.K., Rao, A.K., Venkatasubbaiah, K.: Spatio-temporal growth of disturbances in a boundary layer and energy based receptivity analysis. Phys. Fluids **18**, 094101 (2006)
34. Sommerfeld, A.: Ein Beitrag zur hydrodynamiscen Erklärung der turbulenten Flussigkeitsbewegung. In: Proceedings of 4th International Congress Mathematicians, Rome, pp. 116–124 (1908)
35. Sundaram, P., Sengupta, T.K., Bhaumik, S.: The three-dimensional impulse response of a boundary layer to different types of wall excitation. Phys. Fluids **30**, 124103 (2018)
36. Tollmien, W.: Über die enstehung der turbulenz. I. English translation: NACA TM 609 (1931)
37. Trefethen, L.N., Trefethen, A.E., Reddy, S.C., Driscoll, T.A.: Hydrodynamic stability without eigenvalues. Science **261**(5121), 578–584 (1993)
38. Van Der Pol, B., Bremmer, H.: Operational calculus based on two-sided Laplace integral. Cambridge University Press, Cambridge, UK (1959)
39. Yeo, K.S., Zhao, X., Wang, Z.Y., Ng, K.C.: DNS of wavepacket evolution in a Blasius boundary layer. J. Fluid Mech. **652**, 333–372 (2010)